

Nuclear Quadrupole Moment of ^{119}Sn Giampaolo Barone,^{*,†} Remigius Mastalerz,[‡] Markus Reiher,^{*,‡} and Roland Lindh^{*,§}

Dipartimento di Chimica Inorganica e Analitica, Università di Palermo, Viale delle Scienze, Parco d'Orleans II, 90128 Palermo, Italy, Laboratorium für Physikalische Chemie, ETH Zurich, Hönggerberg Campus, Wolfgang-Pauli-Strasse 10, CH-8093 Zurich, Switzerland, and Department of Theoretical Chemistry, Chemical Center, Lund University, P.O.B. 124, 221 00 Lund, Sweden

Received: October 27, 2007; In Final Form: December 7, 2007

Second-order scalar-relativistic Douglas–Kroll–Hess density functional calculations of the electric field gradient, including an analytic correction of the picture change error, were performed for 34 tin compounds of which molecular structures and ^{119}Sn Mössbauer spectroscopy parameters are experimentally known. The components of the diagonalized electric field gradient tensor, V_{xx} , V_{yy} , V_{zz} , were used to determine the quantity V , which is proportional to the nuclear quadrupole splitting parameter ΔE . The slope of the linear correlation plot of the experimentally determined ΔE parameter versus the corresponding calculated V data allowed us to obtain an absolute value of the nuclear quadrupole moment Q of ^{119}Sn equal to $Q = 13.2 \pm 0.1 \text{ fm}^2$. This is about 11% larger than the picture-change-error-affected value and in good agreement with previous estimates of the picture change error in compounds of similar atomic charge. Moreover, despite the variety of the tin compounds considered in this study, the new result is in excellent agreement with the previously determined most accurate value of Q for ^{119}Sn of $Q = 12.8 \pm 0.7 \text{ fm}^2$, but with a noticeably narrower error bar. The reliability of the calibration method in the calculation of the ΔE parameter of tin compounds is within a margin of $\pm 0.3 \text{ mm s}^{-1}$ when compared to experimental data and does not depend on the inclusion of the picture change correction in the density functional calculations but is essentially determined by the use of an atomic natural orbital relativistic core-correlated basis set for the description of the core electron density. The results obtained suggest that the present picture-change-corrected Douglas–Kroll–Hess approach provides reliable electric field gradients in the case of closed-shell metal compounds involving elements up to the fifth row of the periodic table for which spin–orbit coupling is negligible.

1. Introduction

Mössbauer spectroscopy is a valuable tool to provide support for the structure determination of tin compounds. Information about the oxidation state of a particular tin species can be obtained by exploiting the isomer shift, which appears due to different valence electron configurations. Nuclei with nuclear spin states higher than $I > 1/2$ exhibit a charge distribution, which is not spherically symmetric and gives rise to an electric nuclear quadrupole moment. In the case of an asymmetric electronic charge distribution the nuclear quadrupole moment interacts with the electric field gradient (EFG). The nuclear quadrupole moment can be determined efficiently by a joint application of theoretical calculations and experiments. It has been recently shown that EFG calculations based on density functional theory (DFT) can be employed routinely for supporting the structure determination of arbitrary tin compounds by means of the ^{119}Sn nuclear quadrupole splitting parameter ΔE .^{1,2} A calibration function was obtained by taking advantage of the linear correlation of experimental ΔE parameters and the corresponding calculated EFG data, which was used to determine the nuclear quadrupole moment Q of ^{119}Sn and a theoretical ΔE parameter of a specific tin compound. The linear relation between Q and ΔE is given by eq 1 where V_{xx} , V_{yy} , V_{zz}

$$\Delta E = \frac{1}{2}eQV_{zz}\sqrt{\left(1 + \frac{1}{3}\eta^2\right)} = \frac{1}{2}eQV \quad (1)$$

are the components of the diagonalized EFG tensor chosen such that $|V_{zz}| \geq |V_{yy}| \geq |V_{xx}|$. The asymmetry parameter η is given by $\eta = (V_{xx} - V_{yy})/V_{zz}$, e represents the elementary charge, and the quantity V is defined as $V = V_{zz}(1 + \eta^2/3)^{1/2}$. For our study we choose 34 mononuclear tin compounds, with an overall size of 15–95 atoms and various coordination numbers in oxidation states II or IV. For all compounds under investigation solid-state structures and ^{119}Sn experimental Mössbauer parameters are known.^{1,2} The molecular structures are depicted in Figures 1–3.

A previous study² revealed that the inclusion of kinematic relativistic effects on the wave function through the Douglas–Kroll–Hess (DKH) Hamiltonian^{3–6} significantly improved the agreement between the experimental and theoretical values of the splitting parameter ΔE compared to nonrelativistic results. This already facilitated quantitative predictions of the ^{119}Sn Mössbauer nuclear quadrupole splitting parameter for a variety of tin compounds.² In particular, a detailed analysis of the linear correlation uncovered that the use of the atomic natural orbital relativistic core correlated (ANO-RCC) all-electron basis set for the tin atom, compared to a nonrelativistic DZVP basis set, increased the correlation coefficient of the fit from 0.982 to 0.996. This can be attributed to the improved description of the electronic charge distribution of the core region by the ANO-RCC basis set, which was designed for second-order DKH

* Corresponding authors. G.B. e-mail: gbarone@unipa.it. M.R. e-mail: markus.reiher@phys.chem.ethz.ch. R.L. e-mail: roland.lindh@teokem.lu.se.

† Università di Palermo.

‡ ETH Zurich.

§ Lund University.

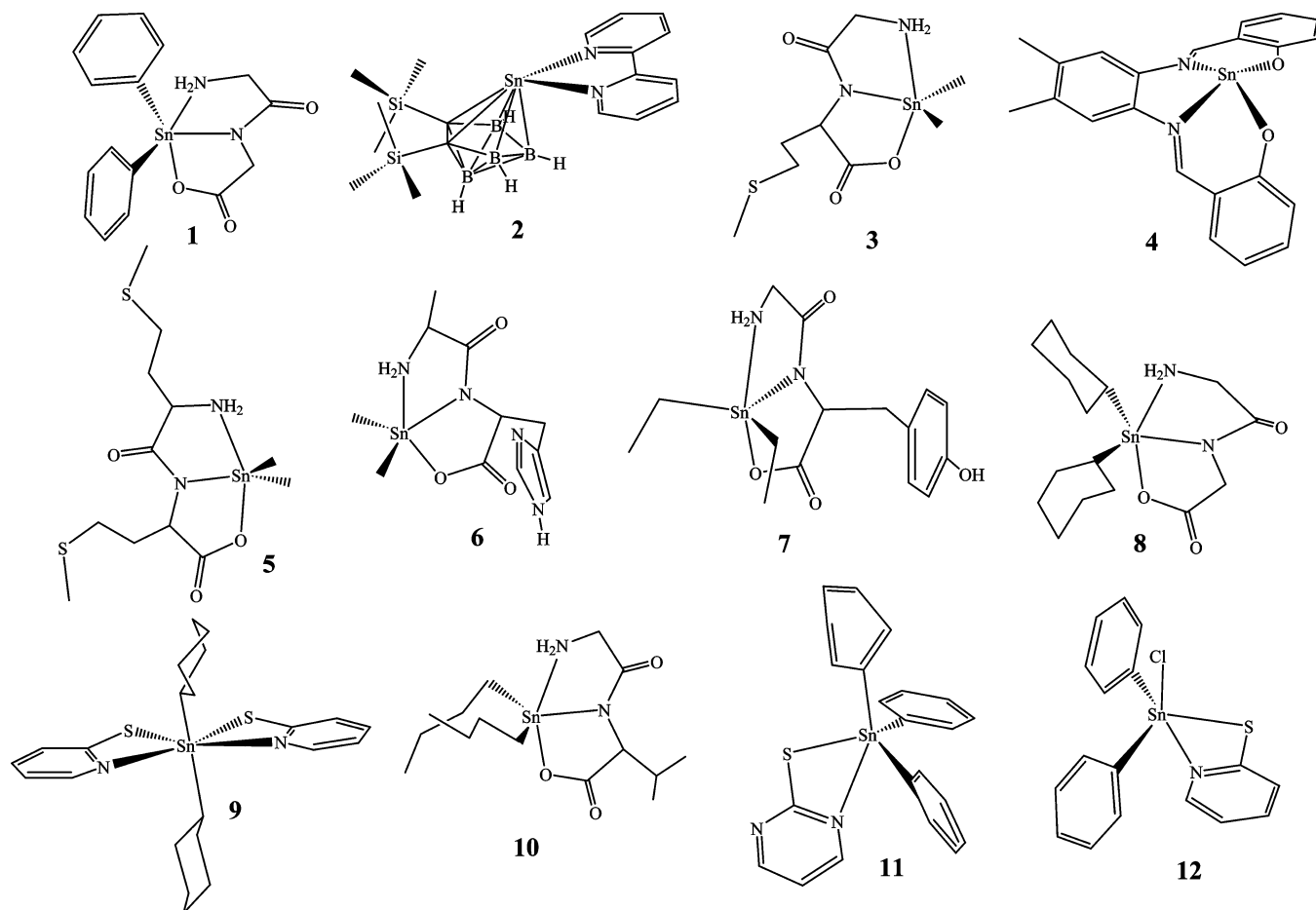


Figure 1. Molecular structures of compounds 1–12.

calculations. Moreover, the relativistic corrections significantly influenced the slope of the linear trend, which allowed us to obtain an estimate of the nuclear quadrupole moment of $Q = 11.9 \pm 0.1 \text{ fm}^2$, which is in good agreement with the experimentally determined one of $Q = 10.9 \pm 0.8 \text{ fm}^2$ ⁷ as well as with the currently most accurate theoretical value for ^{119}Sn of $Q = 12.8 \pm 0.7 \text{ fm}^2$,^{8,9} obtained by Svane et al.⁹ by solid-state DFT calculations on simple model systems. The study of Svane et al. demonstrates once more that the most reliable way to determine nuclear quadrupole moments is to combine the EFG obtained from quantum chemical calculations with experimental data.^{8,10}

Preceding studies verified that the discrepancy between calculated and experimental ΔE parameters^{1,2} does not depend on the deviation between the solid-state and the calculated isolated molecules and that a structure optimization in a nonrelativistic framework already furnishes a satisfying agreement with the experimental structures.¹ Previous investigations also point out that further improvements should include corrections of the so-called picture-change effect (see below).²

It must, however, be emphasized that the previous studies focused on the accuracy of the calculated splitting parameter ΔE and on its application to the structural determination of medium to large size tin compounds. In this respect the picture change affected approach already provided valuable support for the structural characterization of any type of tin compound by ^{119}Sn Mössbauer spectroscopy and is useful in particular for the structure determination of tin compounds for which X-ray crystallography cannot be performed.

To proceed forward to an even more accurate determination of the nuclear quadrupole moment Q , it is necessary to include

an analytical correction of the so-called picture change error. This error is a consequence of using the nonrelativistic expression for the EFG operator within the DKH approach.^{11,12} The mathematical formalism of Dirac's relativistic theory of the electron requires the wave function to be composed of four-component spinors. In a fully relativistic four-component framework a one-electron term of the total electronic contribution to the expectation value of the EFG, $\langle V_{ij}^1 \rangle$, with $i, j = x, y, z$, is obtained in first-order perturbation theory,

$$\langle V_{ij}^1 \rangle = \langle \psi_{\text{D}} | V_{ij}^1 | \psi_{\text{D}} \rangle \quad (2)$$

Here, ψ_{D} denotes the unperturbed one-electron Dirac-like 4-spinor, which can be subdivided into a so-called large component (ψ_{L}) and a small component (ψ_{S}). The Douglas–Kroll–Hess transformation technique provides a unitary transformation U , which eliminates the small component ψ_{S} of the original one-electron spinor and yields a transformed two-component orbital ϕ_{L} according to

$$U\psi_{\text{D}} = U \begin{pmatrix} \psi_{\text{L}} \\ \psi_{\text{S}} \end{pmatrix} = \begin{pmatrix} \phi_{\text{L}} \\ 0 \end{pmatrix} \quad (3)$$

The same unitary transformation U must also be applied to the EFG operator in each one-electron matrix element, as illustrated by the following equation,

$$\langle V_{ij,\text{DKH}\infty}^1 \rangle = \langle U\psi_{\text{D}} | UV_{ij}^1 U^\dagger | U\psi_{\text{D}} \rangle = \langle \phi_{\text{L}} | V_{ij,\text{DKH}\infty}^1 | \phi_{\text{L}} \rangle \quad (4)$$

If the transformation of the EFG operator is skipped, the expectation value of the EFG is afflicted by a systematic flaw called picture change error.

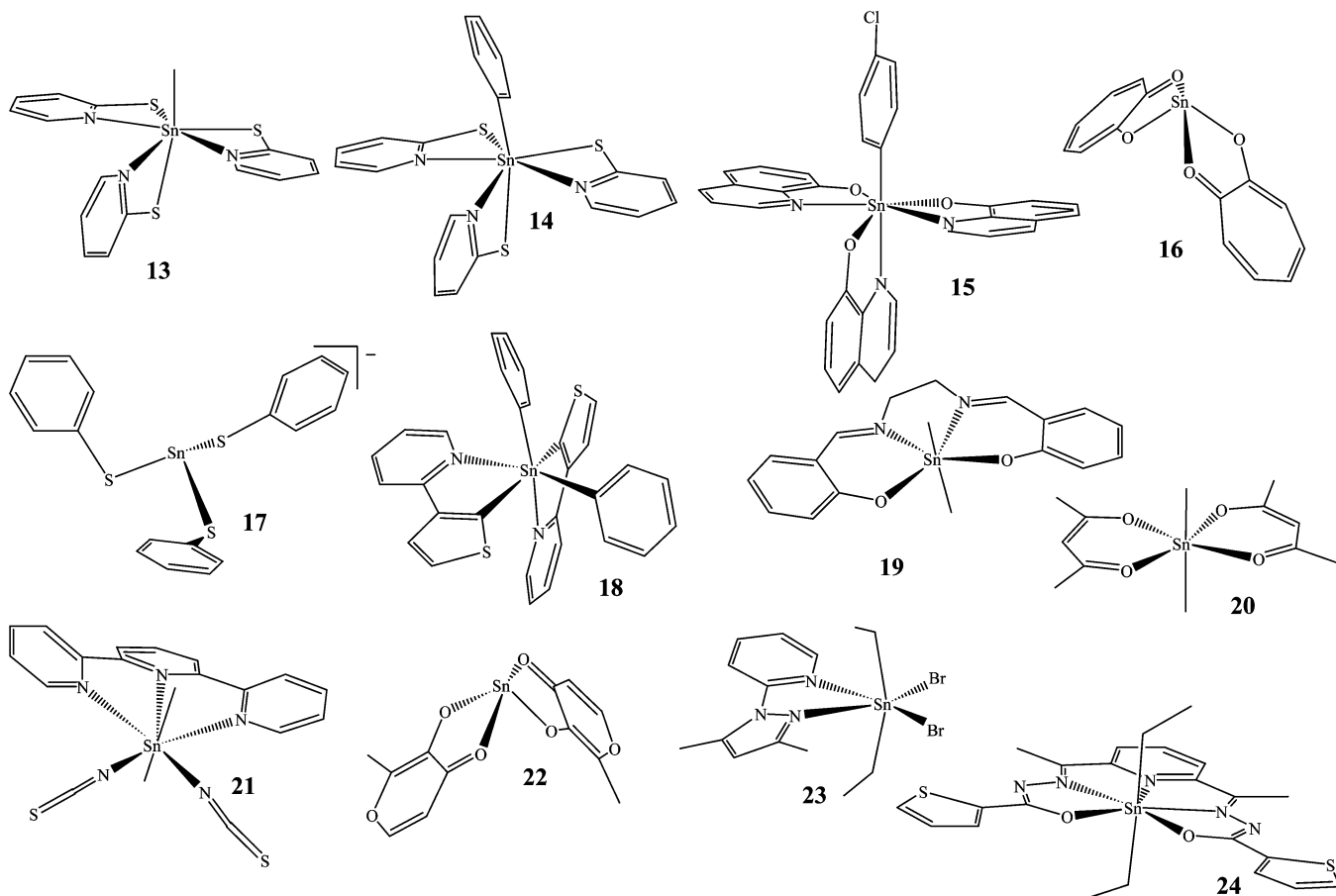


Figure 2. Molecular structures of compounds 13–24.

The development of an analytical picture-change-corrected arbitrary-order DKH unitary transformation scheme for one-electron operators has been the subject of recent work that provided a systematic approximation hierarchy for the desired expectation value.^{13,14} Following this approach, a one-electron molecular orbital integral of the total electronic contribution to the EFG at a specific nucleus $\langle V_{ij}^1 \rangle$ can be expressed as

$$\langle V_{ij}^1(n,m) \rangle = \left\langle \phi_L^{\text{DKH}n} \left| \sum_{k=0}^m V_{ij,c,k}^1 \right| \phi_L^{\text{DKH}n} \right\rangle \quad (5)$$

where n and m refer to the DKH transformation order of the Hamiltonian and of the EFG operator, respectively. A generalization of the calculation of the EFG to the N -electron case is straightforward, because the one-electron operator V_{ij}^1 needs to be replaced by a sum of N such one-electron operators, where N is the number of occupied orbitals.

We have recently published a comprehensive study on EFGs in hydrogen halides obtained with the above-mentioned picture-change-corrected analytical high-order DKH method.¹⁵ Particularly interesting for the present study are the results obtained for hydrogen iodide, because iodine and tin are neighbors in the periodic table. It has been shown that for closed-shell molecules up to the atomic number of iodine spin-orbit effects are likely to be negligible.¹⁵ A comparison with Dirac–Hartree–Fock calculations, close to the basis set limit, reveals an increase in the expectation value of the EFG at the iodine nucleus by about 17% compared to the nonrelativistic Hartree–Fock results. A scalar-relativistic DKH(2,2) approach, which is of second order in both orbital and property transformation yields a deviation of only 0.01 au ($\approx 0.1\%$) in comparison to the EFG

obtained by a Dirac–Hartree–Fock reference calculation.¹⁵ The picture change error was quantified to be about 11% for the EFG on the iodine nucleus.¹⁵ According to these results a relativistic treatment of core properties avoiding the picture change error is mandatory also for tin compounds. Referring to the results obtained for the iodine nucleus, a DKH(2,2) approach can be regarded as a suitable choice for a picture-change-effect-free calculation of the EFG in tin compounds. In this respect the implementation of the arbitrary-order DKH property module¹⁴ in the Molcas program package^{16,17} has promoted the determination of a more accurate value of the nuclear quadrupole moment of ^{119}Sn , which is the subject of the present paper.

2. Computational Details

In this work we use a DKH formalism in which all spin-dependent terms have been neglected. Therefore, we obtain a so-called scalar-relativistic one-component DKH model, which is the standard implementation of the DKH approach. The calculation of the electric field gradient at the tin nucleus in compounds 1–34 was performed with the scalar-relativistic DKH(2,2) and DKH(4,2) approaches in a DFT framework employing the B3LYP¹⁸ density functional and an ANO-RCC^{19,20} basis set. The basis set of the tin atom was contracted to 6s5p3d1f, for all other atoms a contraction level of VDZP quality was used. The structures of the compounds involved in this study were the nonrelativistic DFT/DZVP fully optimized geometries previously reported.¹ The eigenvalues V_{ii} of the diagonalized EFG tensor, with $i = x, y, z$ were used to derive the quantity V , which is related to the theoretical quadrupole splitting parameter ΔE as defined by eq 1. All calculations were carried out with the Molcas-7.0^{16,17} software package.

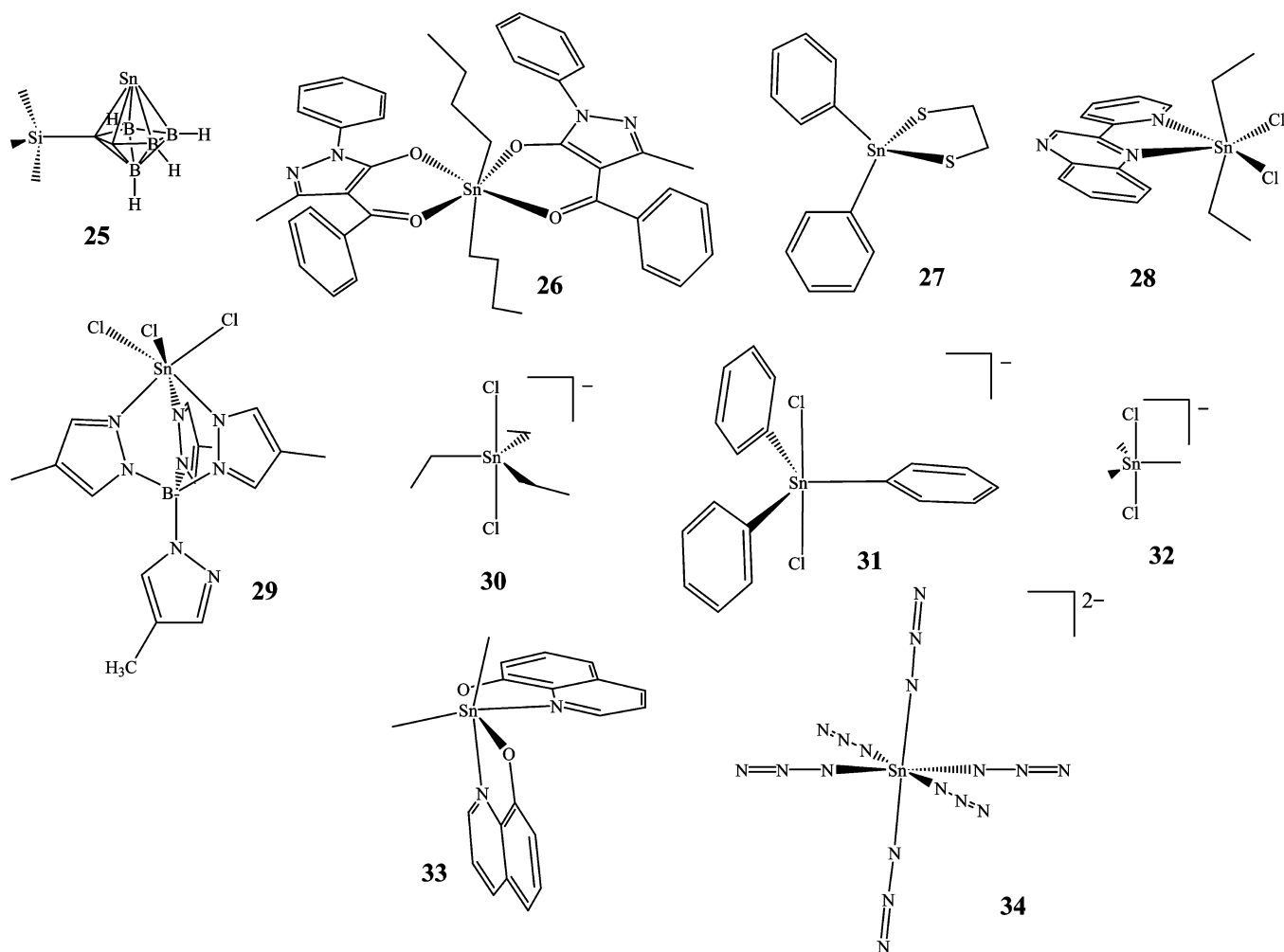


Figure 3. Molecular structures of compounds 25–34.

3. Results and Discussion

The ^{119}Sn Mössbauer parameters η , V_{zz} , and V obtained from DKH–DFT calculations and the experimental ΔE values are reported in Table 1. The experimental splitting parameter ΔE for each Sn compound under investigation was taken from ref 1 and references therein, respectively. The 34 tin compounds were mainly selected on the basis of their experimental ΔE values,¹ covering the range analyzed (-3.5 to $+4.3$ mm s^{-1} ; see Figure 4). Their Mössbauer spectra were recorded at liquid nitrogen or liquid helium temperatures (see ref 1 and references therein). Their structures, experimentally determined by X-ray crystallography, have been previously optimized within non-relativistic DFT.¹ To minimize structural contributions due to the solid-state packing, only tin compounds showing monomer units in the crystallographic unit cell have been selected. In fact, average deviations of about 3% were observed between calculated and experimental structures.¹ Moreover, it was shown that the scattering of the data points in the linear correlation plot did not depend on the observed discrepancies between the solid-state and the calculated structures.¹

The nuclear quadrupole moment of ^{119}Sn was determined by plotting the experimental ΔE data versus the corresponding V parameter of compounds 1–34 and exploiting the linear relation of ΔE and the nuclear quadrupole moment Q as illustrated in eq 1. According to eq 1 the slope of this linear correlation plot is given by $1/2eQ$, from which Q can easily be extracted. The advantage of a linear regression is that a large variety of

compounds with different molecular structures can be used to determine Q and therefore method inherent errors in the calculation of V are likely to cancel out if they affect the various Sn molecules in different ways. After having determined the nuclear quadrupole moment Q by this procedure one can obtain a theoretically calculated ΔE parameter from eq 1 for each Sn compound under study. The correlation plots of the experimentally determined ΔE parameter versus the corresponding values of V for compounds 1–34, without (i.e., DKH(2,0)) and with (i.e., DKH(2,2)) the inclusion of the picture change corrections are shown in Figure 4.

A single remarkable deviation from the linear trend indicated by a triangle symbol on the right-hand side of the line in Figure 4 was due to compound 2, which has been observed before.² The occurrence of this outlier has been associated with the singlet–triplet state nature of the electronic structure of this compound, which shows up mainly due to the presence of the 2,2′-bipyridine ligand.² However, the investigation of multireference or open-shell compounds like 2 would require the inclusion of spin–orbit effects in the computational method. As a consequence we have excluded the data point associated with compound 2 from the linear regression analysis of the data. The linear fit considering the remaining 33 data points produced a slope of 0.805 ± 0.014 $\text{mm s}^{-1} \text{ au}^{-1}$ with a linear correlation coefficient of $R = 0.995$. Using the slope as a calibration constant it is possible to calculate the quadrupole splitting

TABLE 1: ^{119}Sn Mössbauer Parameters Obtained from Scalar-Relativistic DFT Calculations on Compounds 1–34

no.	η^a	V_{zz}^a	V^b	ΔE^c	$\Delta E_{\text{calcd}}^d$	$\Delta E_{\text{calcd}}^e$
1	0.62	-2.84	-3.02	-2.24	-2.43	-2.46
2	0.54	4.77	4.99	(+)2.73	4.02	3.96
3	0.65	-3.01	-3.21	(-)2.53	-2.59	-2.57
4	0.53	1.99	2.08	(+)1.34	1.67	1.65
5	0.68	-2.99	-3.21	(-)2.94	-2.58	-2.57
6	0.58	-3.03	-3.20	(-)3.20	-2.58	-2.57
7	0.71	-3.22	-3.48	(-)2.87	-2.81	-2.78
8	0.71	-3.21	-3.47	(-)3.11	-2.79	-2.80
9	0.58	3.35	3.54	(+)2.84	2.85	2.85
10	0.74	-3.13	-3.40	(-)2.65	-2.74	-2.73
11	0.21	-1.92	-1.93	(-)1.65	-1.56	-1.60
12	0.99	2.81	3.24	(+)2.58	2.61	2.65
13	0.06	2.71	2.71	(+)2.23	2.18	2.20
14	0.15	2.61	2.62	(+)1.89	2.11	2.14
15	0.06	2.14	2.14	(+)1.71	1.73	1.74
16	0.63	2.44	2.60	(+)1.98	2.09	2.07
17	0.00	1.68	1.68	(+)1.38	1.36	1.33
18	0.29	-1.22	-1.24	(-)0.73	-1.00	-0.99
19	0.13	4.76	4.77	(+)3.46	3.84	3.84
20	0.12	5.12	5.13	(+)3.93	4.14	4.13
21	0.28	4.77	4.83	(+)4.29	3.89	3.86
22	0.64	2.63	2.80	(+)1.99	2.25	2.24
23	0.08	4.60	4.60	(+)4.00	3.71	3.73
24	0.15	4.91	4.92	(+)3.72	3.97	3.94
25	0.65	4.13	4.41	(+)2.79	3.55	3.48
26	0.06	5.27	5.28	(+)4.14	4.25	4.26
27	0.58	-1.93	-2.04	(-)1.56	-1.64	-1.65
28	0.05	4.62	4.63	(+)3.98	3.73	3.75
29	0.19	-0.09	-0.09	(-)0.43	-0.07	-0.08
30	0.00	-3.89	-3.89	-3.49	-3.14	-3.18
31	0.00	-3.54	-3.54	-3.02	-2.85	-2.90
32	0.00	-3.70	-3.70	-3.31	-2.98	-3.01
33	0.48	2.63	2.73	+2.06	2.20	2.19
34	0.00	0.00	0.00	0.00	0.00	0.00

^a $\eta = (V_{xx} - V_{yy})/V_{zz}$ with $|V_{zz}| \geq |V_{yy}| \geq |V_{xx}|$. ^b $V = V_{zz}(1 + \eta^2/3)^{1/2}$ in atomic units. ^c Experimental nuclear quadrupole splitting parameter (in mm s^{-1}) from the literature (see ref 1). The sign in brackets is added to ΔE following the sign of V according to DFT calculations. ^d ΔE_{calcd} is the quadrupole splitting parameter calculated with the DKH(2,2) model by exploiting the slope of the linear fit in Figure 4. ^e Quadrupole splitting parameter calculated with the DKH(2,0) approach.²

parameter ΔE from the data for V for each of the compounds investigated,

$$\Delta E_{\text{calcd}} = 0.805V \pm 0.28 \text{ mm s}^{-1} \quad (6)$$

where the error bar is the average mean square error for the 33 compounds and represents the precision within which the ΔE parameter can be calculated. The calculations of the EFG were carried out with the DKH(2,2) approach. To assess the accuracy of the results obtained with the DKH(2,2) model, we performed DKH(4,2) calculations of the same property for the six smallest compounds investigated, i.e., compounds **16**, **22**, **25**, **30**, **32**, and **34**. The DKH(4,2) results essentially coincide with the DKH(2,2) ones. In fact the V parameters for the six smallest compounds obtained with the DKH(4,2) model are almost identical to those obtained with the DKH(2,2) approach with differences in the third decimal place. This result is in perfect agreement with those obtained for HI, for which the difference in the principal component of the EFG tensor V_{zz} at the iodine nucleus, comparing the DKH(2,2) and DKH(4,2) models, shows up in the third decimal place.¹⁵

As expected, the linear correlation coefficient of $R = 0.995$ is very similar to the one determined ignoring a picture change correction,² namely, $R = 0.996$. As already mentioned, this has to be attributed to the good quality of the ANO-RCC basis set.

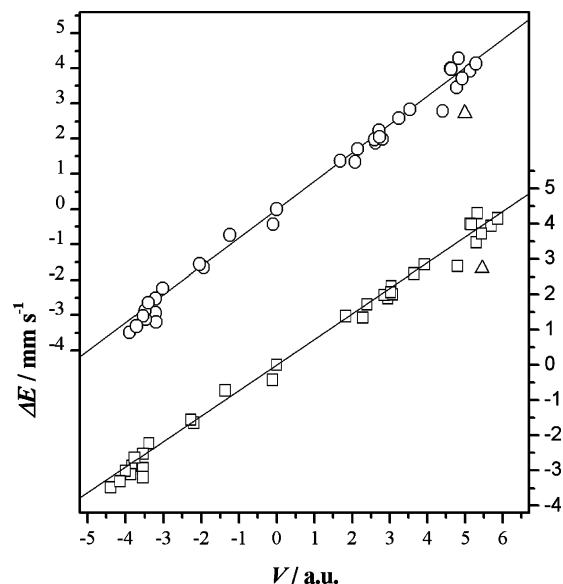


Figure 4. Correlation plot of experimental ΔE data versus the corresponding theoretically calculated V parameter, obtained from picture-change-error-free DKH(2,2) (spheres) and DKH(2,0) (squares) DFT calculations for compounds 1–34 (see Table 1). The triangle symbols correspond to compound 2, which was excluded from the data set. The solid lines are least-squares linear regressions over 33 points (see text).

TABLE 2: Estimates of the Nuclear Quadrupole Moment (NQM) of ^{119}Sn Selected from the Literature

method	NQM	published by
experimental	$10.9 \pm 0.8 \text{ fm}^2$	Haas et al. ⁷
solid-state DFT	$12.8 \pm 0.7 \text{ fm}^2$	Svane et al. ⁹
nonrelativistic DFT	$15.2 \pm 4.4 \text{ fm}^2$	Barone et al. ¹
DKH(2,0) DFT	$11.9 \pm 0.1 \text{ fm}^2$	Krogh et al. ²
DKH(2,2) DFT	$13.2 \pm 0.1 \text{ fm}^2$	this work

Of course the excellent linear correlation of the picture-change-affected data is due to the fact that the picture change error can be regarded as a systematic error of constant magnitude, which affects every component of the diagonalized EFG tensor in the same way. In the calculation of the asymmetry parameter $\eta = (V_{xx} - V_{yy})/V_{zz}$, the picture change error simply results in a scaling factor for the numerator and denominator, which finally cancels out. The calculation of the parameter $V = V_{zz}(1 + \eta^2/3)^{1/2}$ is thus only affected by the picture change in V_{zz} , resulting in a constant shift of V , which will not affect the linear correlation of the data points.

The good agreement of the picture-change-affected estimates of the ΔE parameter with the experimental ones has also to be attributed to an error cancellation. The calculation of the nuclear quadrupole moment Q from experimental ΔE data and picture-change-affected V parameters leads to a picture-change-affected Q , which again was used in combination with the corresponding picture-change-affected V parameter to obtain the theoretical estimates of ΔE . Because both quantities Q and V were affected by a picture change error of about the same magnitude but opposite sign, the picture change error approximately cancels out in the calculation of the splitting parameter ΔE . As far as the determination of an accurate value of the nuclear quadrupole moment Q is concerned, the picture-change correction is essential. Table 2 presents an overview of the nuclear quadrupole moment of ^{119}Sn obtained by experiment and theory.

The value obtained in the present work of $Q = 13.2 \pm 0.1 \text{ fm}^2$ compared to the previously estimated quadrupole moment of $Q = 11.9 \pm 0.1 \text{ fm}^2$ ² is in much better agreement with the

reference data of $Q = 12.8 \pm 0.7 \text{ fm}^2$ as provided by refs 8 and 9. Note that our result also features a considerably smaller error bar. This improvement is remarkable considering the size and variety of the tin compounds investigated. It is important to mention that the updated values of both V_{zz} and of V decrease by an amount of $10 \pm 1\%$ compared to the previously published picture-change-affected data,² and that the new value of the quadrupole moment Q is 11% higher than the picture-change-error-affected result. Concerning the latter point, we recall that by using the slope of the linear plot as a calibration constant only the absolute value of Q can be determined, though it is known from experiment that Q is negative for ^{119}Sn .^{7–9} As a consequence the new value of Q drops to $Q = -13.2 \pm 0.1 \text{ fm}^2$, resulting in a decrease of about 11% in comparison to the picture-change-affected value of $Q = -11.9 \pm 0.1 \text{ fm}^2$.² These results are in excellent agreement with those recently obtained for hydrogen iodide,¹⁵ where a decrease of 11% for V_{zz} was observed upon correction for the picture change error. The difference in the slope of the linear correlation plot of ΔE and V comparing the picture-change-corrected and picture-change-affected results² is due to the updated value of the nuclear quadrupole moment. The change in the slope of the correlation plot amounts to about 11%, reflecting the change of the picture in the determination of the nuclear quadrupole moment.

The picture-change-corrected DKH(2,2) DFT results closely resemble those recently determined for iodine with a DKH(2,2) Hartree–Fock framework.¹⁵ These results suggest that (i) the present approach allows us to cover all necessary relativistic corrections in the calculation of the nuclear quadrupole moment of ^{119}Sn and (ii) the corresponding value of Q reported in ref 8 should be updated. The DKH(2,2) method can thus be regarded to provide reliable electric-field-like properties of closed shell compounds involving elements up to the fifth row of the periodic table, for which spin–orbit coupling can be neglected (see discussion above).

Recently, an alternative approach to the direct evaluation of the nuclear quadrupole moment by using relative instead of absolute values of the EFG was presented by Belpassi et al.²¹ for cases where DFT calculations of the field gradient reveal serious shortcomings. It turned out that this approach leads to stable results for the nuclear quadrupole moment in a variety of gold compounds. We should emphasize in this context that this procedure may improve estimates for the nuclear quadrupole moment of transition metal compounds, but for closed-shell compounds of main group elements like tin absolute values of the EFG proved to yield reliable results for the nuclear quadrupole moment.

A final argument related to the relativistic quantum chemical calculation of core properties concerns the size of the chemical compounds considered in the present work. For example, compound **26** consists of 95 atoms and 963 basis functions were used in the calculation of the EFG at the tin nucleus. Due to the computational cost associated with all-electron relativistic calculations only small tin compounds like SnY_4 or SnY_3 ($Y = \text{H}, \text{CH}_3, \text{C}_2\text{H}_5, \text{F}, \text{Cl}, \text{Br}, \text{I}, \text{At}$), or $\text{Me}_{4-n}\text{SnX}_n$ ($X = \text{Cl}, \text{Br}, \text{I}; n = 1 - 3$) have been considered so far in the literature.^{22–24} To study valence properties of larger systems, relativistic effective core potentials were used in conjunction with non-relativistic DFT calculations.²⁵ Finally, configuration interaction studies of valence properties of SnTe and SnTe^+ have also been reported using relativistic effective core potentials.²⁶ Efficient resolution of the identity schemes like the Cholesky decomposition²⁷ are therefore needed to reduce the computational demand of density functional calculations on large compounds. The

application of the Cholesky decomposition in the calculation of the two-electron integrals of compound **26**, for instance, accelerated the calculation by a factor of about 60. The numerical values of η , V_{zz} , and V obtained coincide with those reported in Table 1, showing differences in V of only 2 units in the sixth decimal digit. This encouraging result demonstrates that the Cholesky decomposition approach yields accurate wave functions and thus electric field gradients as compared to a conventional implementation.

4. Conclusion

The EFG tensor at the tin nucleus in 34 different tin compounds was correlated to the corresponding experimental ^{119}Sn Mössbauer quadrupole splitting values, as defined in eq 1, to obtain a calibration function, given by eq 6, from which an accurate nuclear quadrupole moment of ^{119}Sn as well as reliable values of the nuclear quadrupole splitting parameter for a diverse set of tin compounds could be predicted. The inclusion of picture change corrections within a DKH(2,2) model in the DFT calculations has furnished a value of the nuclear quadrupole moment of ^{119}Sn equal to $Q = 13.2 \pm 0.1 \text{ fm}^2$. Due to the smaller error bar this value coincides well with $Q = 12.8 \pm 0.7 \text{ fm}^2$, which up to now was considered the most accurately determined value. Our results suggest that all scalar-relativistic corrections to electric-field-like properties in arbitrary closed-shell compounds of the fifth row of the periodic table can be recovered by the presented approach. Moreover, our results once more demonstrate that ^{119}Sn Mössbauer spectroscopy in combination with reliable quantum chemical calculations can serve as a suitable instrument to provide benchmark data for testing the performance of state-of-the-art quantum chemical methods in the calculation of chemical core properties for medium to large size compounds. An extension of this work to the calculations of Mössbauer parameters of iron compounds is in progress in our laboratories.

Acknowledgment. Financial support from the University of Palermo and provision of computer resources from the LU-NARC computer center of Lund University are gratefully acknowledged. R. M. and M. R. thank the Schweizer National Fonds (Project no. 200021-113479/1) for generous financial support.

References and Notes

- (1) Barone, G.; Silvestri, A.; Ruisi, G.; La Manna, G. *Chem. Eur. J.* **2005**, *11*, 6185–6191.
- (2) Krogh, J. W.; Barone, G.; Lindh, R. *Chem. Eur. J.* **2006**, *12*, 5116–5121.
- (3) Douglas, M.; Kroll, N. M. *Ann. Phys.* **1974**, *82*, 89–155.
- (4) Hess, B. A. *Phys. Rev. A* **1986**, *33*, 3742–3748.
- (5) Wolf, A.; Reiher, M.; Hess, B. A. *J. Chem. Phys.* **2002**, *117*, 9215–9226.
- (6) Reiher, M.; Wolf, A. *J. Chem. Phys.* **2004**, *121*, 2037–2047.
- (7) Haas, H.; Menningen, M.; Andreasen, H.; Damgaard, S.; Grann, H.; Pedersen, F. T.; Petersen, J. W.; Weyer, G. *Hyperfine Interact.* **1983**, *15/16*, 215–218.
- (8) Pyykkö, P. *Mol. Phys.* **2001**, *99*, 1617–1629.
- (9) Svane, A.; Christensen, N. E.; Rodriguez, C. O.; Methfessel, M. *Phys. Rev. B* **1997**, *55*, 12572–12577.
- (10) Alonso, R. E.; Svane, A.; Rodriguez, C. O.; Christensen, N. E. *Phys. Rev. B* **2004**, *69*, 125101.
- (11) Baerends, E. J.; Schwarz, W. H. E.; Schwerdtfeger, P.; Snijders, J. G. *J. Phys. B: At. Mol. Opt. Phys.* **1990**, *23*, 3225–3240.
- (12) Kellö, V.; Sadlej, A. J. *Int. J. Quantum Chem.* **1998**, *68*, 159–174.
- (13) Wolf, A.; Reiher, M. *J. Chem. Phys.* **2006**, *124*, 064102.
- (14) Wolf, A.; Reiher, M. *J. Chem. Phys.* **2006**, *124*, 064103.
- (15) Mastalerz, R.; Barone, G.; Lindh, R.; Reiher, M. *J. Chem. Phys.* **2007**, *127*, 074105.

- (16) Veryazov, V.; Widmark, P.-O.; Serrano-Andres, K.; Lindh, R.; Roos, B. O. *Int. J. Quantum Chem.* **2004**, *100*, 626–635.
- (17) Karlström, G.; Lindh, R.; Malmqvist, P.-A.; Roos, B. O.; Ryde, U.; Veryazov, V.; Widmark, P.-O.; Cossi, M.; Schimmelpfennig, B.; Neogrady, P.; Seijo, L. *Comput. Mater. Sci.* **2003**, *28*, 222–239.
- (18) Becke, A. D. *J. Chem. Phys.* **1993**, *98*, 5648–5652.
- (19) Roos, B. O.; Lindh, R.; Malmqvist, P.-A.; Veryazov, V.; Widmark, P.-O. *J. Phys. Chem. A* **2004**, *108*, 2851.
- (20) Roos, B. O.; Lindh, R.; Malmqvist, P.-A.; Veryazov, V.; Widmark, P.-O. *J. Phys. Chem. A* **2005**, *109*, 6575–6579.
- (21) Belpassi, L.; Tarantelli, F.; Sgamellotti, A.; Götz, A.; Visscher, L. *Chem. Phys. Lett.* **2007**, *442*, 233–237.
- (22) Lie, W.; Fedorov, D. G.; Hirao, K. *J. Phys. Chem. A* **2002**, *106*, 7057–7061.
- (23) Giju, K. T.; Proft, F. D.; Geerlings, P. *J. Phys. Chem. A* **2005**, *109*, 2925–2936.
- (24) Bagno, A.; Casella, G.; Saielli, G. *J. Chem. Theor. Comput.* **2006**, *2*, 37–46.
- (25) Schmatz, S.; Ebker, C.; Labahn, T.; Stoll, H.; Klingenberg, U. *Organometallics* **2003**, *22*, 490–498.
- (26) Giri, D.; Pati, K.; Das, K. K. *J. Chem. Phys.* **2006**, *124*, 154301.
- (27) Aquilante, F.; Pedersen, T. B.; Lindh, R. *J. Chem. Phys.* **2007**, *126*, 194106.